sustainability

MDPI

Article

Finite Element Simulation of Total Nitrogen Transport in Riparian Buffer in an Agricultural Watershed

Xiaosheng Lin [1,2], Jie Tang [1,2,*], Zhaoyang Li [2] and Haiyi Li [2]

[1] Key Lab of Groundwater Resources and Environment, Ministry of Education, Jilin University, Changchun 130000, China; shuihaizi115@163.com

[2] College of Environment and Resource, Jilin University, Changchun 130000, China; zhaoyang@jlu.edu.cn (Z.L.); lhy334@126.com (H.L.)

* Correspondence: tangjie@jlu.edu.cn; Tel.: +86-0431-8515-9440

Academic Editor: Marc A. Rosen

Received: 10 February 2016; Accepted: 15 March 2016; Published: 22 March 2016

Abstract: Riparian buffers can influence water quality in downstream lakes or rivers by buffering non-point source pollution in upstream agricultural fields. With increasing nitrogen (N) pollution in small agricultural watersheds, a major function of riparian buffers is to retain N in the soil. A series of field experiments were conducted to monitor pollutant transport in riparian buffers of small watersheds, while numerical model-based analysis is scarce. In this study, we set up a field experiment to monitor the retention rates of total N in different widths of buffer strips and used a finite element model (HYDRUS 2D/3D) to simulate the total N transport in the riparian buffer of an agricultural non-point source polluted area in the Liaohe River basin. The field experiment retention rates for total N were 19.4%, 26.6%, 29.5%, and 42.9% in 1,3,4, and 6m-wide buffer strips, respectively. Throughout the simulation period, the concentration of total N of the 1mwide buffer strip reached a maximum of 1.27 mg/cm^3 at 30 min, decreasing before leveling off. The concentration of total N about the 3mwide buffer strip consistently increased, with a maximum of 1.05 mg/cm^3 observed at 60 min. Under rainfall infiltration, the buffer strips of different widths showed a retention effect on total N transport, and the optimum effect was simulated in the 6mwide buffer strip. A comparison between measured and simulated data revealed that finite element simulation could simulate N transport in the soil of riparian buffer strips.

Keywords: finite element model; rainfall infiltration; pollutant retention; numerical modeling; agricultural watershed

1. Introduction

Agricultural non-point source pollution has emerged as a major source of pollution in water environments worldwide. Surface and subsurface runoff is a major mechanism for transporting sediments, fertilizers and pesticides to ground or surface water [1]. Organic forms and inorganic forms of N are transported with sediments and debris. Once released into the soil, N is transported with water and is discharged into rivers, leading to the eutrophication of rivers [2]. Use of fertilizers adds nitrate, ammonium, or various forms of organic N, including urea, to agricultural watersheds. Total N is often adopted to indicate N load in water bodies that are being investigated [3].

The Liaohe River basin (in the southwest of Northeast China) is one of the seven biggest basins in China. The distribution of surface runoff in the study area is corresponsive to precipitation. The river is recharged by groundwater as well as the slow flow in rainfall periods, while there is an even no flow recharge in dry periods [4]. With the stimulation of groundwater discharge, the runoff losses of nitrogen is 2088.39 t/a [5]. Consequently, the key problem in the Liaohe River basin is to address water pollution [6].

The establishment of riparian buffers can mitigate agricultural non-point source pollution in watersheds [7]. Width is an important factor which could determine the effects of pollutant reduction of a buffer strip. Castelle *et al.* designed different buffer widths ranging from 3 to 200 m that proved the buffer width effects depending on site-specific conditions [8]. More field experiments have been conducted to simulate pollutant transports in different widths of riparian buffers [9–11]. Those studies concluded that the wider filter strips could remove more total N discharged into the water body, and the reduction rate ranged from 30%~80% in different regions [12,13].

Numerous studies have investigated the pollutant transports in soils of riparian buffers at the watershed level, and many mathematical simulation models have been developed [14]. Some environment models could be used to simulate soil water infiltration [15]. An effective evaluation of Water Erosion Prediction Project (WEPP) has been proposed for grass buffer strips in controlling runoff and sediment resistance [16,17]. However, solute transport in unsaturated soil is affected by complex factors, such as soil heterogeneity, natural boundary conditions, and solute transport parameters, and so on. There are different methods used to solve flow and solute problems and usually these problems must be solved numerically [18]. Theoretical numerical models are used, such as FEFLOW, which is an advanced finite element subsurface flow and transport modeling system with an extensive list of functionalities [19]. Zhang *et al.* estimated a simultaneous velocity vector and water pressure head which can be used as direct input to transport models [8]. Moreover, the popular Visual Modflow, which is used to simulate groundwater flow and contaminant transport, by using the fully 3D finite differential method [20].

The numerical models mainly include finite difference (FD) and finite element (FE) methods. The difference of the FD method and FE method is that FD requires an iterative solution even for a linear problem, and its computation takes more time when compared with the FE method. The FD method suffers from low flexibility in terms of subdivision mesh, and thus proves to be ineffective in resolving complicated boundary conditions [21]. FE method is the main stream of numerical analysis methods applicable to arbitrary geometry and boundary conditions, material and geometric nonlinear problems, as well as anisotropic problems [22]. It is effective in solving boundary conditions and initial value problems in three-dimensional unsaturated flow under complex geometry [23]. A number of studies have proved that FE programs such as HYDRUS and Seep/w, which can accurately simulate water, energy, and solute transport in saturated and unsaturated porous media by using soil physical parameters [24]. The process of rainfall infiltration into unsaturated soil is complex due to the number of soil parameters involved, and the casual nature of water flow boundary conditions. The Richards' equation is the most rigorous way to describe interaction between unsaturated and saturated zones [25–27]. In particular, the Hydrus package is a one-dimensional, two-dimensional and three-dimensional FE computer model that is obtained by combining Darcy-Buckingham's law [28], and it ignores the effect of air on soil water movement and solves the governing equation for water flow by using a modified form of the Richards' equation.

When designing uniform riparian buffers with appropriate models, the major difficulty lies in decisions about their actual width. In this study, we conducted a field experiment to monitor the retention rate of total N increased with the width of agriculture riparian buffer. Thereafter, a finite element model was developed for simulating the spatial variation of total N transport through the riparian buffer.

Core ideas:

- Total N transport through riparian buffer was simulated by a finite element model.
- The retention rate of total N increased with the width of buffer strips.
- The highest rate was detected in a 6m-wide buffer strip.
- Finite element simulation could be adopted to simulate N transport in riparian buffer strips.

2. Materials and Methods

2.1. Study Site

The study site is located in the Liaohe River Basin (E 123°18′–125°36′, N42°36′-44°10′) in Jilin Province, Northeast China (Figure 1). This basin covers an area of 15,746 km^2 and constitutes an important part of China's major commodity-grain planting base. The main agricultural use in the river basin is primarily for tillage crops, specifically corn and soybeans. The upper reaches are the segment above Erlongshan Reservoir, which is a low-mountain and hilly area with an altitude from 200 to 600 m. The middle reaches are the section from the Erlongshan Reservoir downwards to Chengzishang Hydrological Station, which is a hilly area with an altitude from 100 to 300 m. The lower reaches are the section from Chengzishang Hydrological Station downwards to the Sanjiangkou iron bridge on the Siping-Qiqihar railway line [26]. The whole river basin primarily consists of Loamy soils and the average slope is 8%. The annual mean temperature is 6.25 °C and annual average precipitation and evaporation figures are 450–700 mm and 700–1020 mm, respectively (2010–2014) (China Meteorological Data sharing Service System [29]). The climate change in the East Liaohe River Watershed of Jilin Province is controlled by Pacific low-pressure and Siberian high-pressure [30]. The upstream is rich in forest resources, which constitutes the main water resource for its residents, while the downstream area is based largely on agro-pastoral industry, rendering the whole region to be the main recipient of pollutant emission.

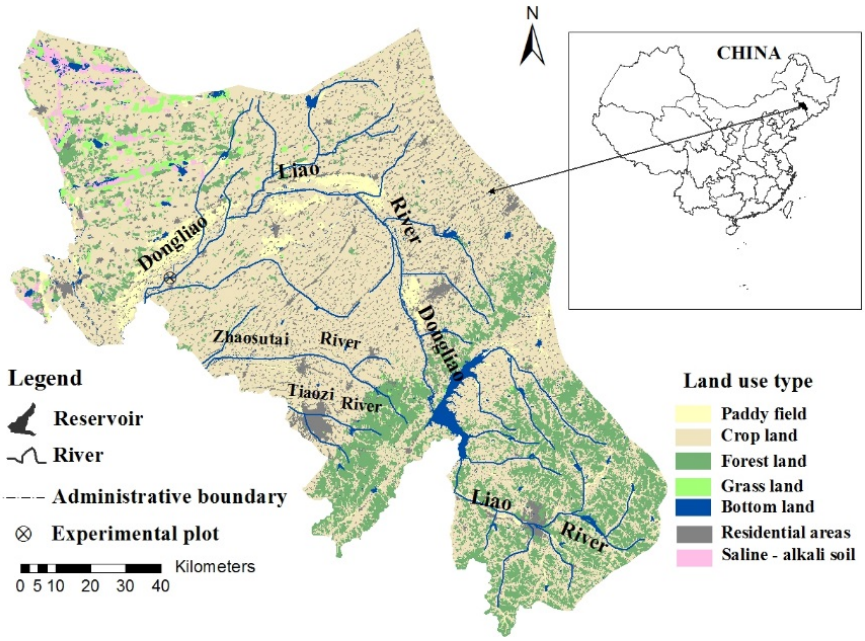

Figure 1. Location of the study area in the Liaohe River Basin, Jilin Province, Northeast China.

2.2. Field Experiments

Field experiments were conducted on vacant land downstream of the basin. The land was a 120 m^2 area adjacent to the riverbank with small amounts of grass. Crops were cultivated in the neighboring field. Experiments were performed to monitor the retention rate of total N in the soil of the riparian buffer under rainfall infiltration. Four buffer widths of 1, 3, 4, and 6 m were set up in the study area, in which 1- and 3-m-wide buffer strips were used to validate the results of model simulations.

The pollutant retention experiments were established as follows (Figure 2): A reservoir was set up between the river and experiments sites. Water was pumped from the river to a reservoir and dispersed into the experiments sites by flow pipes, where a pump was installed in the bottom of

the reservoir to regulate the flow rate. Therefore, the flow rate was controlled at a constant 1.5 L/s. The reservoir was a water storage tank made of polyethylene and the experiments site had a steady flow slot made of white steel. We collected a 0–20 cm depth of undisturbed soil and covering the slot as the buffer strip soil. The duration of flow lasted 60 min. When the water flowed through the outlet, timing commenced, with samples collected at 5 min, 10 min, 20 min, 30 min, 40 min, 50 min and 60 min. At the same time, we also collected the inlet water samples from the reservoir as a control group. In total, 32 samples were collected using 500-mL plastic bottles, preserved by adjusting pH to 1–2 with concentrated sulfuric acid (1.84 g/mL), and stored at −20 °C. Total N concentration was determined using alkaline potassium persulfate digestion spectrometry [31].

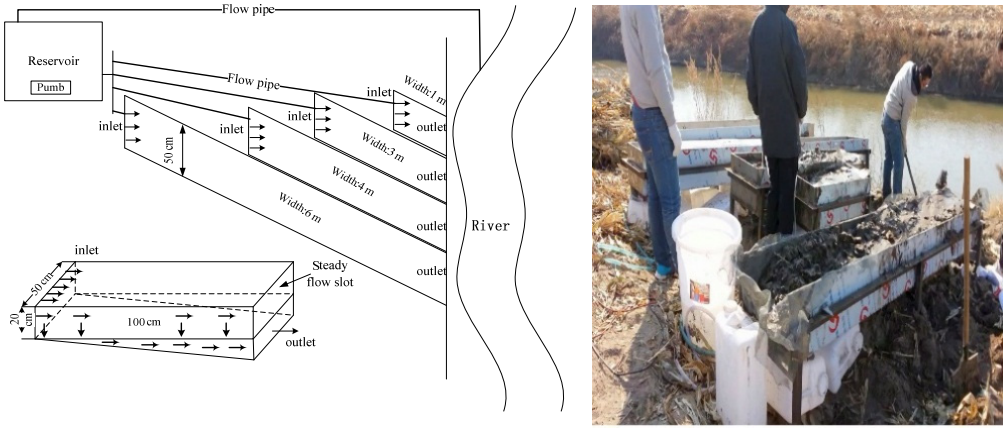

Figure 2. Diagram (**left**) and photograph (**right**) of the field experiment design.

In the field experiment, the removal efficiency in % (R) for N analysis in the buffer zone was calculated according to:

$$R = \frac{C_{\text{in}} - C_{out}}{C_{in}} \times 100\% \quad (1)$$

where C_{in} (mg/cm^3) and C_{out} (mg/cm^3) are concentration of the control group and the experiments sample in the inlet and outlet, respectively.

2.3. Numerical Simulation

The FE method discretizes the continuous solution domain into a set of finite number of units, then uses the approximate function hypothesized within each unit to differently express the unknown field function to be solved in the entire solution domain. It calculates the approximate value of the field function within each unit by using the interpolation function, in order to obtain the approximate value of the field function in the entire solution domain [32].

2.4. Model Parameter Settings

In this study, we used a modified Richards' equation to describe soil water flow. This equation can effectively express two-dimensional and three-dimensional flow motion in stable saturated–unsaturated porous media [33].

$$\frac{\partial \theta}{\partial t} = \frac{\partial}{\partial X_i}\left[K\left(K_{ij}^A \frac{\partial h}{\partial X_j} + K_{ij}^A\right)\right] - S \quad (2)$$

where θ is volumetric water content (L^{3}L^{-3}); h is pressure head (L); K_{ij}^A is dimensionless expression of anisotropic tensor; t is time (min); S is sedimentation coefficient (T^{-1}); K is unsaturated hydraulic conductivity (T^{-1}); and X_i is spatial coordination (i = 1, 2, 3) [L].

The HYDRUS 2D/3D software simulates soil water retention curve on the basis of Van Genuchten-Mualem's equation [34,35]:

$$S_{\mathrm{e}}(h) = \left[1 + (\alpha h)^n\right]^{-m} \tag{3}$$

$$K(S_e) = K_s S_e^l \left[1 - \left(1 - S_e^{l/m}\right)^m\right]^2 \tag{4}$$

where S_{e} is effective water content, $\frac{\theta - \theta_r}{\theta_s - \theta_r}$ $(0 \leqslant S_{\mathrm{e}} \leqslant 1)$; θ_r is remaining water content; θ_s is the saturated water content; α and n are curve shape parameters; $m = 1 - \frac{1}{n}$; K_s is the saturated hydraulic conductivity of the soil (cm/min); and l is an empirical fitting parameter, typically 0.5 [36].

We chose total soil N as the pollutant to establish the mathematical model of saturated–unsaturated solute transport in the soil [24]:

$$\frac{\partial(\theta c)}{\partial \mathrm{t}} = \frac{\partial\left(\theta D_{ij} \frac{\partial c}{\partial X_j}\right) - \partial(q_i c)}{\partial X_i} \tag{5}$$

where D_{ij} is diffusion coefficient (cm^2/d); c is solution mass concentration ($\mathrm{g/cm}^3$); q_i is water flux (cm/d); and X_i is spatial coordination (i = 1, 2, 3) [L].

Equation (3) was used to calculate flow motion in the three-dimensional horizontal cross-section, wherein X_i = x represents the horizontal axis; X_i = y represents the vertical axis; and X_i = z represents the anterior–posterior axis.

2.5. Boundary Condition Settings

We simulated N transport in two buffer strips with different widths: 1 m (X, Y, and Z = 100 cm, 100 cm, and 20 cm) and 3 m (X, Y, and Z = 100 cm, 300 cm, and 20 cm). The mesh design and boundary conditions of the FE model are shown in Figure 3 (an example of the 1-m-wide buffer strip). Triangular prism meshes were discretized to generate the optimal FE model.

Boundary conditions of the model were set as follows: with the blue color indicating the constant flux; bright green was set to the atmospheric boundary; dark green on the slope surface was set as seepage face and grey was set to no flux. A total of six observation nodes (N1–N6) were set up to measure total N content (Figure 3).

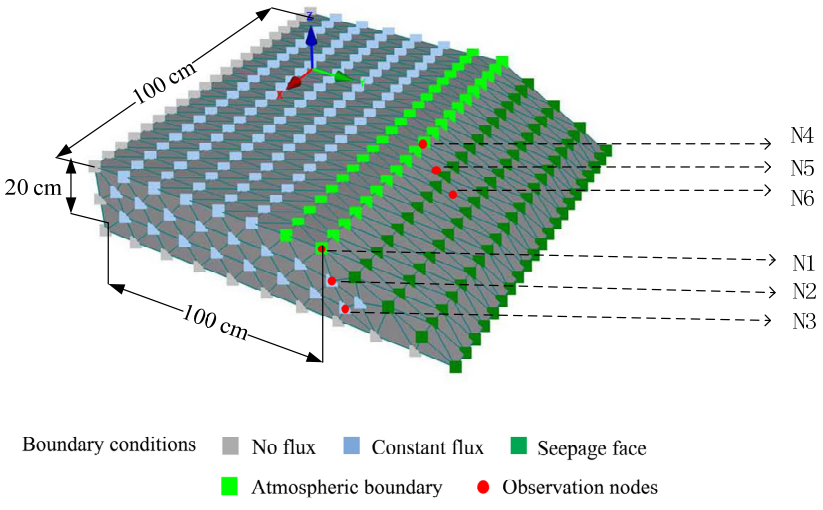

Figure 3. Mesh design and boundary conditions of the finite element model.

2.6. Model Parameter Values

Surface soil samples (depth: 0–20 cm) were collected in the experiments site to measure soil bulk density, field capacity (θ_r) and saturated soil moisture content (θ_s) in the laboratory. We collected samples in the river to measure the total N concentration as solute concentration. Other hydraulic parameters for water flow and solute transport parameters were taken from the soil catalog provided by the HYDRUS software [37] and the results are given in Table 1.

Table 1. Soil water and solute transport parameters.

Water parameters	θ_r (cm^3/cm^3)	θ_s (cm^3/cm^3)	A (cm^{-1})	n	l	K_S (m/s)
	0.1695	0.5091	0.036	1.56	0.5000	0.0173
Solute parameters	D_i (cm)	D_j (cm)	C (mg/cm^3)	Bulk Density (g/cm^3)	Migration Pattern in Fracture Media	-
	0.5	0.1	0.69	1.29	Balanced	-

2.7. Accuracy of Model Simulation

In the simulation, the numbers of nodes for the FE model were 840 and 2400, and the numbers of triangular FE meshes were 1178 and 3563. The maximum iterative time for the 1- and 3-m-wide models was: 1.51×10^1 and 5.16×10^1 s, respectively; and the minimum iterative time was 0.6 s for both models.

As shown in Table 2, the 1- and 3-m-wide models showed a small proportion of variables that could not be explained. Probabilities (Sig.) for the significance test of regression equations were 0.047 and 0.000 (<0.05), indicating that the simulation results are valid.

Table 2. Accuracy test of model simulation by linear regression analysis.

Width	R	R^2	*Adjusted* R^2	*Sig*	n
1 m	0.976	0.951	0.944	0.007	1500
3 m	0.889	0.884	0.883	0.031	1500

2.8. Data Processing

SPSS 17.0 Statistics (SPSS Inc., Chicago, IL, USA) was used for data processing. To check the accuracy of data, the boxplots (Figure 4) were made for the 1- and 3-m-wide buffer strips obtained by model simulation and standard deviation was made for experiments data.

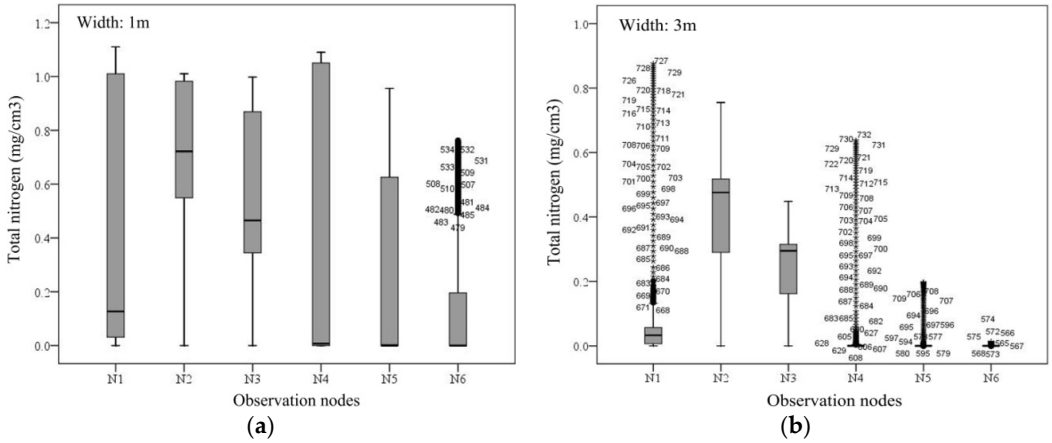

Figure 4. Boxplots of model data. (**A**) 1-m-wide riparian buffer strip and (**B**) 3-m-wide riparian buffer strip.

3. Results

3.1. Retention Capacity of Buffer Strips with Different Widths

The retention rate for total N in the buffer strips changed as a function of time during the rainfall process in the field experiments (Figure 5). In the 1-m-wide buffer strip, the retention rate for total N initially increased from 15.6% at 5 min to a maximum of 19.4% at 30 min; the value then decreased gradually and dropped to 17.2% at 60 min. Similar trends were found in the retention rates for total N of 3- and 4-m-wide buffer strips, which increased as the duration of rainfall erosion increased, from 17.9% and 20.4 at 5 min to 26.6% (3 m) and 29.5% (4 m) at 60 min.

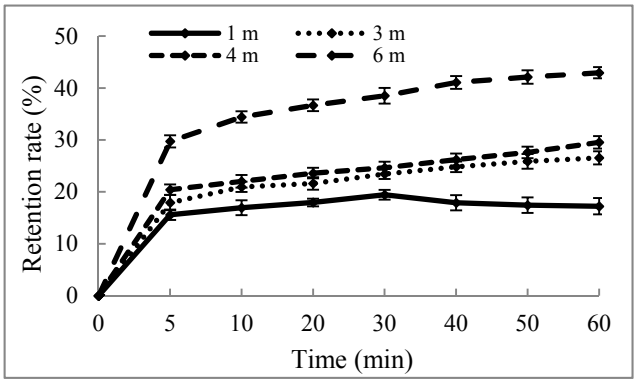

Figure 5. Changes in the retention rate for total nitrogen in riparian buffer strips of different width as a function of rainfall time.

The 6-m-wide buffer strip showed a markedly higher retention capacity than the other buffer strips; its retention rate for total N increased from 29.7% at 5 min to 42.9% at 60 min. The average retention rate of the 6-m-wide buffer strip was 2.3-fold that of the 1-m-wide buffer strip and 1.7- and 1.5-fold those of the 3- and 4-m-wide buffer strips, respectively. This indicates that the 6-m-wide buffer strip had the highest retention capacity for total N throughout the rainfall erosion process.

3.2. Temporal Variation in Total N

Numerical simulation showed the variations in soil solute transport as a function of rainfall time in 2 buffer strips with different width (1 and 3 m, Figure 6). Total N in the soil of the 1-m-wide buffer strip initially increased and then decreased before leveling off, indicating a retention effect of the buffer strip. However, total N constantly increased in the soil of the 3-m-wide buffer strip and did not reach an equilibrium state within 60 min, indicating a trend of further increasing over a longer period.

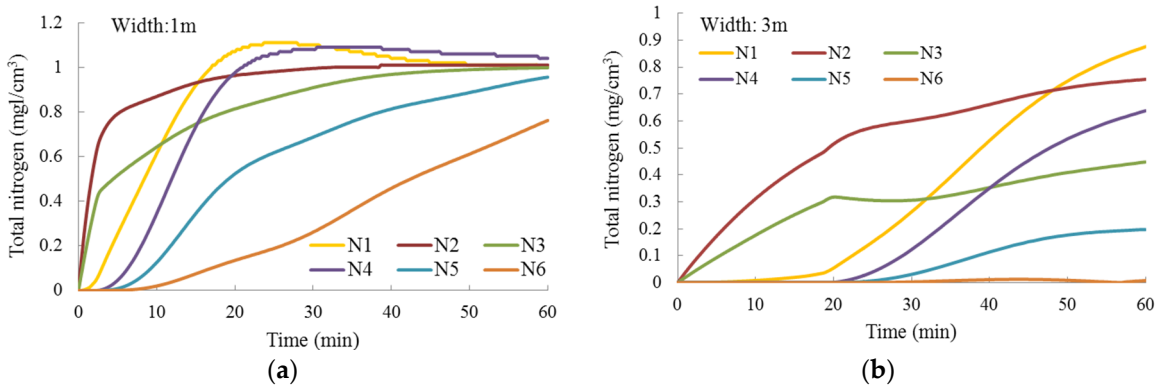

Figure 6. Variations in total N in the soil of 1- and 3-m-wide riparian buffer strips over 60 min of rainfall (measured at 6 observation nodes, N1–N6).

In the 1-m-wide buffer strip, total N reached maximum levels of 1.11 and 1.09 mg/cm^3 at nodes N1 and N4, respectively, after 20 min of rainfall; the maximum levels of total N at nodes N2 (1.01 mg/cm^3) and N3 (0.99 mg/cm^3) were found after 40 min of rainfall. At nodes N5 and N6, total N showed an upward trend after 10 min of rainfall, with the maximum levels of 0.96 and 0.76 mg/cm^3 being found after 60 min of rainfall. The observations of total N transport at the six nodes indicate that total N infiltrated in the soil with rainfall water, from the surface to a greater depth, and from the margin to the interior of the buffer strips.

3.3. Spatial Distribution of Total N

Figure 7 shows the spatial distribution of total soil N content across the 1-m and 3-m-wide riparian buffers. In the 1-m-wide buffer strip, total soil N content initially increased before decreasing over 60 min of rainfall. The highest solute content was 1.27 mg/cm^3 at 30 min of rainfall, and the values decreased thereafter. In the 3-m-wide buffer strip, total soil N content progressively increased over time.

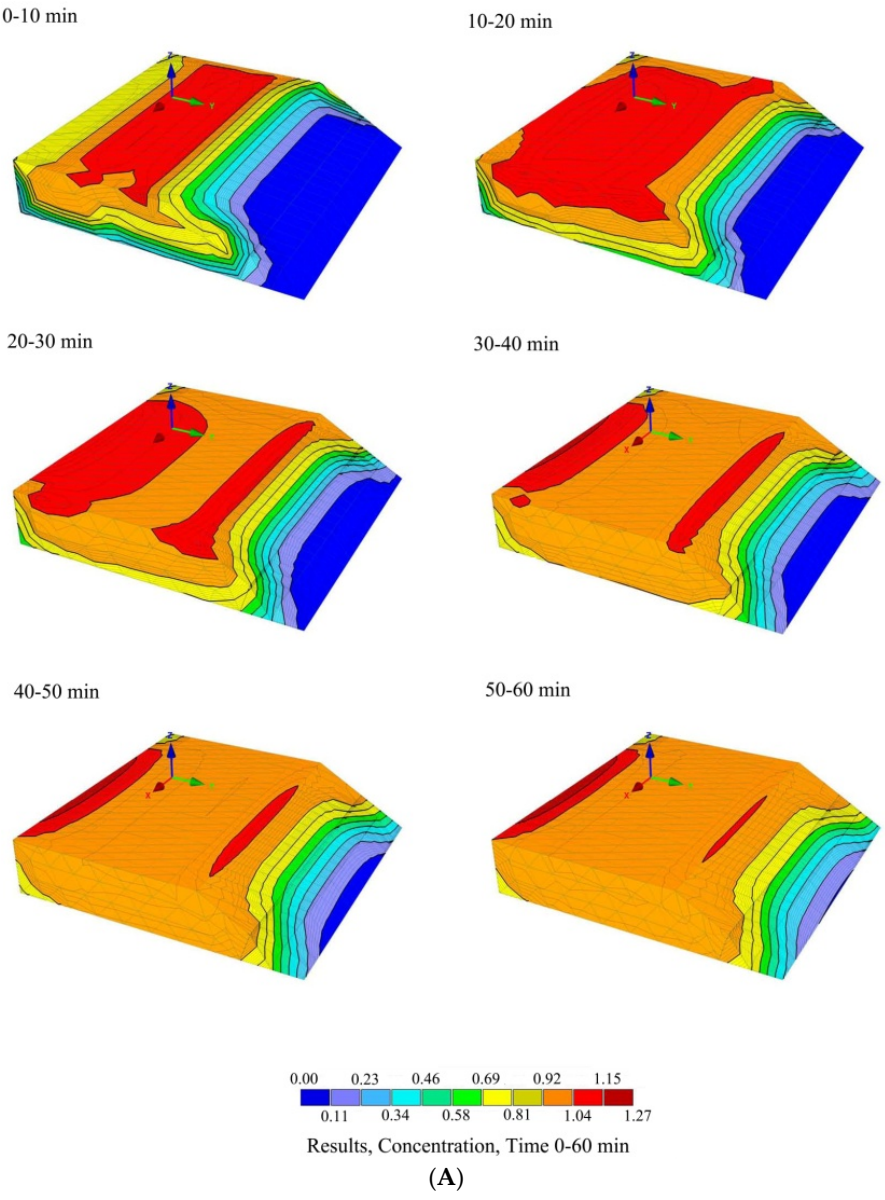

Figure 7. *Cont.*

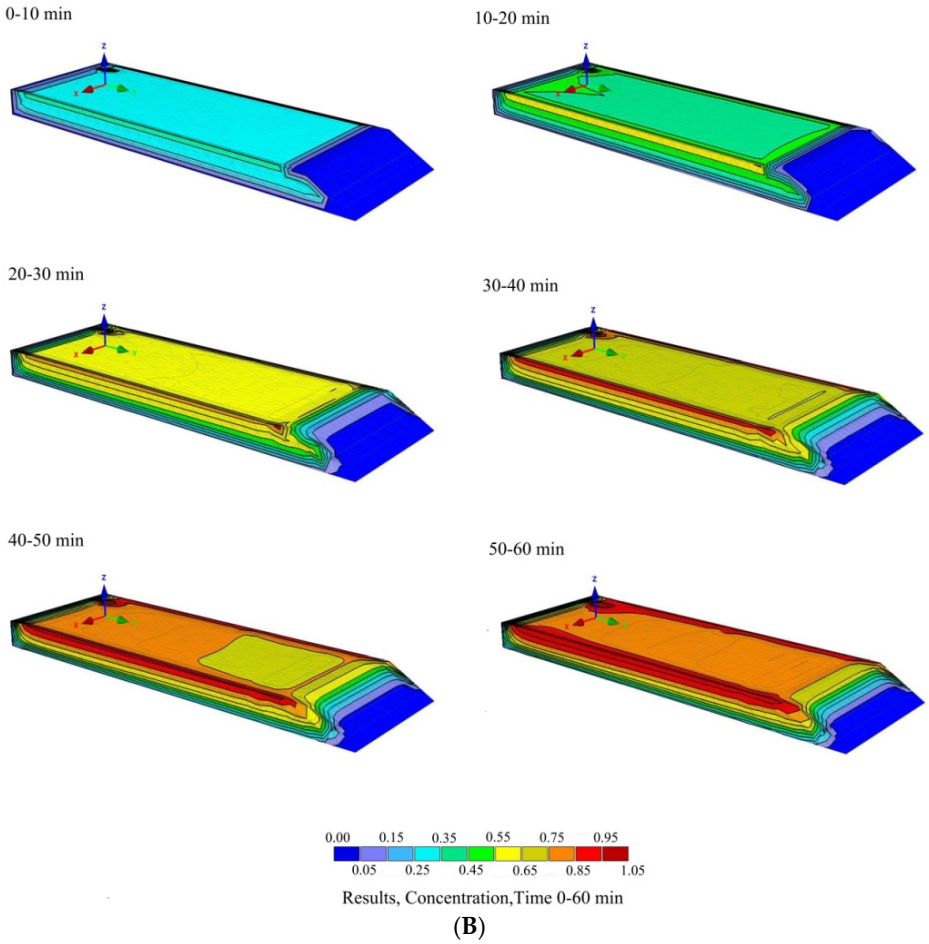

Figure 7. Spatial distribution of total nitrogen in riparian buffer strips over 60 min of rainfall infiltration. (**A**) 1-m-wide riparian buffer strip and (**B**) 3-m-wide riparian buffer strip.

4. Discussion

4.1. Insights on the Retention Capacity of Riparian Buffer Strips

In this study, the field experiment showed that the retention rates for total N were 19.4%, 26.6%, 29.5%, and 42.9% in 1-, 3-, 4-, and 6-m-wide buffer strips, respectively. Other field experiments have also shown that the retention rates for N range from 40% to 94% in buffer strips of 10–60-m width [38–40], and 50% removal efficiencies have been observed in buffers that were approximately 3 m in width [41]. The variability in N retention and removal is due to two factors: variation in the position of the riparian zone with respect to local, intermediate, and regional groundwater flow systems and variation in the hydrogeological properties among riparian zones [41]. For example, high water tables may be found in a buffer in a lower landscape position, which can lead to anaerobic conditions that are more conducive for denitrification. On the other hand, the presence of drains, ditches, and/or movement of groundwater along deep flow paths can allow groundwater to bypass the buffer entirely or decrease denitrification potential [42,43].

A recent study used the riparian ecosystem management model (REMM) to simulate the hydrology and water quality of a field and riparian buffer adjacent to a mangrove wetland in Jobos Bay watershed, Puerto Rico. REMM reduced the total N load by 31%, and a total of 380 kg·N·ha^{-1} was transported in 2008; 13 kg·N·ha^{-1}, in 2009; and 12 kg·N·ha^{-1}, in 2010 [44]. Moreover, NO_3^--N reductions at a second buffer ranged from 76% to 92% across shallow and deeper groundwater, although some of the reduction was probably due to dilution [45].The dilution of NO_3^--N enriched

shallow groundwater can occur if it mixes with deeper groundwater that may upwell near the stream (if a subsurface confining layer is not present or continuous within the buffer) [40]. REMM takes into consideration subsurface flow and sediment yield. Therefore, the model proposed in the present study can be improved by considering slope, groundwater, and sediment yield, in order to achieve a more accurate simulation.

A previous study showed that the impact of riparian buffer zones was clearly observed in higher-order streams where the observed NO_3^- levels are 43.7% less than that of the upland [46]. For buffer site selection, landscape position is a more important defining variable than buffer width if NO_3–N reduction is the primary goal [47]. However, we inferred that buffer site selection should be determined according to different situations: for relatively wide buffers (>30 m), landscape position is the major factor for reducing pollution; for relatively narrow buffers (<15 m), width is a major factor that affects retention capacity.

4.2. Effect of Width on the Retention Capacity of Riparian Buffer Strips

Since narrow buffers were more suitable for our terrain conditions, we studied pollution control in 1-, 3-, 4-, and 6-m-wide buffers in the present study. The 6-m-wide buffer strip showed the highest retention capacity for total N throughout the rainfall erosion process. This is because the water absorption ability of the soil gradually decreased, due to soil moisture increase in buffer strips during rainfall; different equilibrium time for infiltration and saturation led to the variations in the retention rates for total N in the riparian buffers with different widths.

Width is an essential factor that affects the performance of buffers, and it is often related to the composition of the strip [8]. There are contrasting reports about this factor in the literature. Some authors suggest a minimum limit of 10 m [48], while others demonstrate satisfactory results even with 3–5-m-wide buffers [12,49]. Maurizio and Elisa established a buffer composed of a 5-m-wide grass strip and a 1-m-wide row of trees in a private farm in Marano, with maize and wheat cultivated in the neighboring field. The determination of their experiment was that NO_3–N concentrations in the agricultural waters showed that nitrate removal was effective even with buffer strips as narrow as 3 m [50]. The discrepancy in the above results may be due to the different vegetation types used in the buffers.

Plant roots can effectively prevent and absorb pollutants in the soil. Soils with woody vegetation have a higher content of organic matter than soils with grass and shrubs because of the leaves and wood deposited and degraded in the soils [51]. Indeed, 60-m-wide buffers composed of woody soils were more effective in N removal (99.9%) than areas with shrub (83.9%) or grass vegetation (61.6%) [52]. For nitrate however, 20-m-wide woody vegetation showed a good capacity for removing pollutants (65%), while the riparian zone composed of shrubs and grasses did not show good results [53,54]. The abovementioned findings indicate that woody or forest vegetation is suitable for pollutant retention by wider buffers, whereas shrubs and grasses are suitable for narrower buffers. In the present study, we have focused on N retention during the infiltration of rainfall water into the soil. Future studies need to include different vegetation types for thoroughly assessing the retention capacity of riparian buffer strips.

Furthermore, retention rates for total N in buffer strips of different widths showed that total N was affected by the duration of rainfall infiltration in the soil. The soil of the 1-m-wide buffer strip reached an equilibrium state in a short period; thus, the retention rate for total N peaked after 5 min of rainfall and then decreased thereafter. In comparison, the soil of the wider buffer strips (3–6 m) required a longer period to reach equilibrium; as a result, the retention rates for total N gradually increased over time during 60 min of rainfall. Then, do wider buffer strips always have a better retention effect? Historical data show that buffers wider than 7 m produce a marginal increase in terms of Nonpoint-source pollution (NPSP) removal in runoff [55,56]. A recent study has proposed that buffers in row-cropped sites should be 3–4 m in width, whereas buffers in grazed sites should be 15 m in width [57]. In the present study, we only investigated N retention by buffer strips of 1–6 m

in width and assessed the applicability of the proposed model. In our next study, we will combine different types of vegetation to assess the retention capacity of buffers with a wider range of widths and screen the optimal width for buffer strips.

4.3. Social and Economic Implications

Conservation buffers provide a number of benefits to society. Although most conservation practices can benefit both landowners and the public, they also result in some costs. The costs and benefits may not be shared equally by landowners and the public [58]. Meanwhile, farmers, landowners, and non-farm residents express different preferences for the management of agricultural land. Farmers tend to prefer a more neatly manicured setting, while non-farm residents prefer more naturalized settings in rural areas [59–61].

Buffers result in some cost to landowners. Because farming is a tremendously competitive occupation, many farmers feel forced to make management decisions based on short-term profitability, rather than long-term sustainability. For designers, this information suggests that if more attention is paid to the design of conservation buffers, more farmers would be willing plant buffers [62]. Future research efforts that focus on environmental benefits, social and economic issues, and aesthetics and design of buffers offer good opportunities. Scientists need to better understand the ways in which the environmental benefits of buffers interact with economic factors and stakeholder preferences. The implications for policy makers are complex, but equally important.

5. Conclusions

In this study, we used measured data as basic parameters to simulate solute transport in the soil of riparian buffer strips. By using the FE method, we elucidated the patterns of total N transport and pollutant retention in the soil of buffer strips characteristic to the Liaohe River Basin. The results indicate that riparian buffers play a role in the retention of soil pollutants. The width of buffer strips affects the effects of N retention under the same rainfall infiltration conditions. The 6-m-wide buffer strip showed the best retention effect under the experimental conditions. Finite element numerical simulation is accurate in simulating soil pollutant migration in riparian buffers of watersheds. The simulation results provide a reference for the prevention of agricultural non-point source pollution and riparian buffer construction in agricultural watersheds.

Acknowledgments: This study was supported by the National Major Project of Science and Technology on water pollution control and management of China comprehensive treatment technology and research project on Liao river basin (NO.2012 ZX072009).

Author Contributions: Jie Tang and Xiaosheng Lin conceived and designed the experiments; Xiaosheng Lin performed the experiments; Xiaosheng Lin analyzed the data; Zhaoyang Li and Haiyi Li contributed materials; Xiaosheng Lin wrote the paper.

Conflicts of Interest: The authors declare no conflicts of interest.

Abbreviations:

The following abbreviations are used in this manuscript:

N Nitrogen
FE Finite element

References

1. Muscutt, A.D.; Harris, G.L.; Bailey, S.W. Buffer zones to improve water quality: A review of their potential use in UK agriculture. *Agric. Ecosyst. Environ.* **1993**, *45*, 59–77. [CrossRef]
2. Zhang, X.C.; Shao, M.A. The Interacting Models and Mechanisms of Soil Nitrogen with Rainfall and Runoff. *Progress Geogr.* **2000**, *19*, 128–135.

3. Borin, M.; Giupponi, C.; Morari, F. Effects of four cultivation systems for maize on nitrogen leaching: 1-Field experiment. *Eur. J. Agron.* **1997**, *7*, 101–112. [CrossRef]
4. Zhang, L.; Lu, W.X.; Yang, Q.C.; An, Y.K.; li, D.; Gong, L. Hydrological Impacts of Climate Change on Streamflow of Dongliao River Watershed in Jilin Province, China. *Chin. Geogr. Sci.* **2012**, *22*, 522–530. [CrossRef]
5. Liang, D.M. *Study on the Non-Point Source Pollution's Characteristics and Control Technology in Small Watershed—A Case Study of Jilin Section of Liao River*; Jilin University: Changchun, China, 2014.
6. Wang, X.Q.; Zhang, Y.; Liu, C.M. Water quantity-quality combined evaluation method for rivers' water requirements of the instream environment in dualistic water cycle: A case study of Liaohe River Basin. *J. Geogr. Sci.* **2007**, *17*, 304–316. [CrossRef]
7. National Research Council. *Riparian Areas Functions and Strategies for Management*; National Academies Press: Washington, DC, USA, 2002.
8. Castelle, A.J.; Johnson, A.W.; Conolly, C. Wetland and stream buffer size requirement—A review. *J. Environ. Qual.* **1994**, *23*, 878–882. [CrossRef]
9. Xu, Z.; Yang, Z.; Ju, M.; Sheng, Q.W.; Wei, M.S.; Guan, X.X. Nitrogen runoff dominates water nitrogen pollution from rice-wheat rotation in the Taihu Lake region of China. *Agric. Ecosyst. Environ.* **2012**, *156*, 1–11. [CrossRef]
10. Paudel, B.R.; Udawatta, R.P.; Anderson, S.H. Agroforestry and grass buffer effects on soil quality parameters for grazed pasture and row-crop systems. *Appl. Soil Ecol.* **2011**, *48*, 125–132. [CrossRef]
11. Udawatta, R.P.; Kremer, R.J.; Garrett, H.E.; Anderson, S.H. Soil enzyme activities and physical properties in a watershed managed under agroforestry and rowcrop system. *Agric. Ecosyst. Environ.* **2009**, *131*, 98–104. [CrossRef]
12. Dillaha, T.A.; Reneau, R.B.; Mostaghimi, S.; Lee, D. Vegetative filter strips for agricultural nonpoint source pollution control. *Am. Soc. Agric. Eng.* **1989**, *32*, 513–519. [CrossRef]
13. Syversen, N. Effect and design of buffer zones in the Nordic climate: The influence of width, amount of surface runoff, seasonal variation and vegetation type on retention efficiency for nutrient and particle runoff. *Ecol. Eng.* **2005**, *24*, 483–490. [CrossRef]
14. Murray, C.D.; Buttle, J.M. Infiltration and soil water mixing on forested and harvested slopes during spring snowmelt, Turkey Lakes Watershed, central Ontario. *J. Hydrol.* **2005**, *306*, 1–20. [CrossRef]
15. Kroes, J.G. Integrated modeling of the soil-water-atmosphere-plant system using the model SWAP2.0 an overview of theory and an application. *Hydrol. Processes* **2002**, *14*, 1993–2002. [CrossRef]
16. Hayes, J.C.; Dillaha, T.A. *Vegetative Filter Strips. I. Site Suitability and Procedures*; American Society of Agricultural Engineers: St. Joseph, MI, USA, 1992; pp. 92–2102.
17. Laflen, J.M.; Lane, L.J.; Foster, G.R. WEPP, a new generation of erosion prediction technology. *J. Soil Water Conserv.* **1991**, *46*, 34–38.
18. Park, E.; Zhan, H.B. Analytical solutions of contaminant transport from finite one-, two-, and three-dimensional sources in a finite-thickness aquifer. *J. Contam. Hydrol.* **2001**, *53*, 41–61. [CrossRef]
19. Trefry, M.G.; Muffels, C. FEFLOW: A finiteelement ground water flow and transport modeling tool. *Ground Water* **2007**, *45*, 525–528. [CrossRef]
20. Mcdonald, M.G.; Harbaugh, A.; Modflow, W. *Modular Three-Dimensional Finite-Difference Ground-Water Flow Model. 6. Appendix A-1-A-2[R]*; U.S. Geological Survey: Reston, VA, USA, 1999.
21. Nonuo, M. Transient Finite Element Code: A versatile Tool for Well Performance Analyses. Society of Petroleum Engineers. In Proceedings of the Low Permeability Reservoirs Symposium, Denver, CO, USA, 26–28 April 1993.
22. Chen, S.H. Adaptive FEM Analysis for Two-dimension Unconfined Seepage Problems. *J. Hydrodyn.* **1996**, *19*, 60–66.
23. Tan, T.S.; Phoon, K.K.; Chong, P.C. Numerical study of finite element method based solutions for propagation of wetting fronts in unsaturated soil. *J. Geotech. Geoenviron. Eng.* **2004**, *130*, 254–263. [CrossRef]
24. Simunek, J.; Van Genuchten, M.Th.; Sejna, M. *The HYDRUS Software Package for Simulating the Two- and Three-Dimensional Movement of Water, Heat, and Multiple Solutes in Variable-Saturated Media*; University of California: Riverside, CA, USA, 2006.
25. Panday, S.; Huyakorn, P.S. A fully coupled physically-based spatially-distributed model for evaluating surface/subsurface flow. *Adv. Water Resour.* **2004**, *27*, 361–382. [CrossRef]

26. He, Z.; Wu, W.; Wang, S.S. Coupled finite-volume model for 2D surface and 3D subsurface flows. *J. Hydrol. Eng.* **2008**, *13*, 835–845. [CrossRef]
27. Simunek, J.; Van Genuchten, M.T. *The HYDRUS Software Package for Simulating the Two- and Three-Dimen sional Movement of Water, Heat, and Multiple Solutes in Variably-Saturated Media. (Version 2.0)*; Colorado School of Mines Publishers: Golden, CO, USA, 2007.
28. Roberts, T.; Lazarovitch, N.; Warrick, A.W.; Thompson, T.L. Modeling salt accumulation with subsurface drip irrigation using HYDRUS-2D. *Soil Sci. Soc. Am. J.* **2009**, *73*, 233–240. [CrossRef]
29. China Meteorological Data sharing Service System. Available online: http://data.cma.cn (accessed on 14 March 2016).
30. Wen, B.S.; Yan, D.H.; Wang, H.; Liu, J.H.; Yang, Z.Y.; Qin, T.L.; Yin, J. Drought assessment in the Dongliao River basin: Traditional approaches *vs.* generalized drought assessment index based on water resources systems. *Nat. Hazards Earth Syst. Sci.* **2015**, *15*, 1889–1906. [CrossRef]
31. Ministry of Environmental Protection of the People's Republic of China. *National Standard of China, 2012, Determination of HJ 636–2012*; Ministry of Environmental Protection of the People's Republic of China Press: Beijing, China, 2012.
32. GEO-SLOPE International Ltd. *Seepage Modeling with SEEP/W 2007, fourth Edition*; GEO-SLOPE International Ltd.: Calgary, AB, Canada, 2010.
33. Simunek, J.; Van Genuchten, M.T.; Sejna, M. *The HYDRUS Software Package for Simulating Two- and Three-Dimensional Movement of Water, Heat, and Multiple Solutes in Variably Saturated Media, Technical Manual (version 2.0)*; PC Progress: Prague, Czech Republic, 2011.
34. Van Genuchten, M.T. On the accuracy and efficiency of several numerical schemes for solving the convective-dispersive equation. In *Finite Elements in Water Resources*; Pentech Press: London, UK, 1976; pp. 171–190.
35. Van Genuchten, M.T. A closed from equation for predicting the hydraulic conductivity of unsaturated soil. *Soil Sci. Soc. Am. J.* **1980**, *44*, 892–1037. [CrossRef]
36. Mualem, Y. A new model for predicting the hydraulic conductivity of unsaturated porous media. *Water Resour. Res.* **1976**, *12*, 513–522. [CrossRef]
37. Carsel, R.F.; Parrish, R.S. Developing joint probability distributions of soil water retention characteristics. *Water Resour. Res.* **1988**, *24*, 755–769. [CrossRef]
38. Lowrance, R.; Dabney, S.; Schultz, R. Improving water and soil quality with conservation buffers. *J. Soil Water Conserv.* **2002**, *57*, 37A–43A.
39. Stone, K.C.; Hunt, P.G.; Novak, J.M.; Johnson, M.H.; Watts, D.W.; Humenik, F.J. Stream nitrogen changes in an eastern coastal plain watershed. *J. Soil Water Conserv.* **2004**, *59*, 66–72.
40. Osborne, L.L.; Kovacic, D.A. Riparian vegetated buffer strips in water quality restoration and stream management. *Freshwater Biol.* **1993**, *29*, 243–258. [CrossRef]
41. Mayer, P.M.; Reynolds, Jr.; Steven, K.; McCutchen, M.D.; Canfield, T.J. *Riparian Buffer width, Vegetative Cover, and Nitrogen Removal Effectiveness: A Review of Current Science and Regulation*; EPA/600/R-05/118; Environmental Protection Agency: Cincinnati, OH, USA, 2006.
42. Hill, A.R. Nitrate removal in stream riparian zones. *J. Environ. Qual.* **1996**, *25*, 743–755. [CrossRef]
43. Puckett, L.J. Hydrogeologic controls on the transport and fate of nitrate in groundwater beneath riparian buffer zones: Results from thirteen studies across the United States. *Water Sci. Technol. A J. Int. Assoc. Water Pollut. Res.* **2004**, *49*, 47–53.
44. Williams, C.O.; Lowrance, R.; Bosch, D.D.; Williams, J.R.; Benham, E.; Dieppa, A.; Hubbard, R.; Mas, E.; Potter, T.; Sotomayor, D.; *et al*. Hydrology and water quality of a feld and riparian buffer adjacent to a mangrove in Jobos Bay watershed, Puerto Rico wetland in Jobos Bay watershed, Puerto Rico. *Ecol. Eng.* **2013**, *56*, 60–68. [CrossRef]
45. Wiseman, J.D. *Groundwater Nitrate Reductions in a Managed Riparian Buffer Located in the Upper Coastal Plain of North Carolina*; North Carolina State University: Raleigh, NC, USA, 2011.
46. Venkatachalam, A.; Jay, R.; Eiji, Y. Impact of riparian buffer zones on water quality and associated management considerations. *Ecol. Eng.* **2005**, *24*, 517–523. [CrossRef]
47. Johnson, S.R. *An Evaluation of Nitrate Reduction through a Conservation Buffer Upslope of an Established Buffer*; North Carolina State University: Raleigh, NC, USA, 2008.

48. Haycock, N.E.; Pinay, G. Groundwater nitrate dynamics in grass and poplar vegetated riparian buffer strips during the winter. *J. Environ. Qual.* **1993**, *22*, 273–278. [CrossRef]
49. Simmons, R.C.; Gold, A.J.; Groffman, P.M. Nitrate dynamics in riparian forest: Groundwater studies. *J. Environ. Qual.* **1992**, *21*, 659–665. [CrossRef]
50. Maurizio, B.; Elisa, B. Abatement of NO_3–N concentration in agricultural waters by narrow buffer strips. *Environ. Pollut.* **2002**, *117*, 165–168. [CrossRef]
51. Groffman, P.M.; Boulware, N.J.; Zipperer, W.C.; Pouyat, R.V.; Band, L.E.; Colosimo, M.F. Soil nitrogen cycling processes in urban riparian zones. *Environ. Sci. Technol.* **2002**, *36*, 4547–4552. [CrossRef] [PubMed]
52. Aguiar, T.R.; Rasera, K.; Parron, L.M.; Brito, A.G.; Ferreira, M.T. Nutrient removal effectiveness by riparian buffer zones in ruraltemperate watersheds: The impact of no-till crops practices. *Agric. Water Managument.* **2015**. [CrossRef]
53. Young, R.A.; Huntrods, T.; Anderson, W. Effectiveness of vegetated bufferstrips in controlling pollution from feedlot runoff. *J. Environ. Qual.* **1980**, *9*, 483–487. [CrossRef]
54. Douglas-Mankin, K.R.; Daniel, M.N.; Charles, J.B.; Stacy, L.H.; Wayne, A.G. Grass-shrub riparian buffer removal of sediment, phosphorus, and nitrogen from simulated runoff. *J. Am. Water Resour. Assoc.* **2007**, *43*, 1108–1116. [CrossRef]
55. Robinson, C.A.; Ghaffarzadeh, M.; Cruse, R.M. Vegetative filter strip effects on sediment concentration in cropland runoff. *J. Soil Water Conserv.* **1996**, *51*, 227–230.
56. Schmitt, T.J.; Dosskey, M.G.; Hoagland, K.D. Filter strip performance and processes for different vegetation, widths, and contaminants. *J. Environ. Qual.* **1999**, *28*, 1479–1489. [CrossRef]
57. Udawatta, R.P.; Garrett, H.E.; Kallenbach, R.L. Agroforestry Buffers for Nonpoint Source Pollution Reductions from Agricultural Watersheds. *J. Environ. Qual.* **2011**, *40*, 800–806. [CrossRef] [PubMed]
58. Lynch, L.; Brown, C. Landowner decision making about riparian buffers. *J. Agric. Appl. Econ.* **2000**, *32*, 585–596.
59. Ryan, R.L. Local perceptions and values for a midwestern river corridor. *Landsc. Urban Plann.* **1998**, *42*, 225–237. [CrossRef]
60. Nassauer, J.I. Agricultural policy and aesthetic objectives. *J. Soil Water Conserv.* **1989**, *44*, 384–387.
61. Nassauer, J.I. Culture and landscape ecology: Insights for action. In *Placing Nature*; Nassauer, J.I., Ed.; Island Press: Washington, DC, USA, 1997; pp. 1–11.
62. Sarah, T.L.; William, C.S. Environmental benefits of conservation buffers in the United States: Evidence, Promise, and Open questions. *Agric. Ecosyst. Environ.* **2006**, *112*, 249–260. [CrossRef]